Supporting Information

Cu_2O Template Synthesis of High-Performance PtCu Alloy Yolk-Shell Cube Catalysts for Direct Methanol Fuel Cells

Sheng-Hua Ye, Xu-Jun He, Liang-Xin Ding, Zheng-Wei Pan, Ye-Xiang Tong, Mingmei Wu,* Gao-Ren Li*

MOE Laboratory of Bioinorganic and Synthetic Chemistry, *KLGHEI of Environment and Energy Chemistry*, *School of Chemistry and Chemical Engineering, Sun Yat-sen University, Guangzhou 510275, China*

20 August 2020

Note added after first publication: This supplementary information file replaces that originally published on 06 August 2014, in which an incorrect SEM image was included in Figure S1b in error. The correct image is included in this revised version. This does not affect the results or conclusions of the article.

Experimental Section

Electrodeposition of Cu_2O yolk-shell cubes and the synthesis of PtCu alloy yolk-shell cubes. All chemical reagents were analytical grade, and they were used directly without any purification. Ti sheets as substrate were prepared complying the following steps before each experiment: firstly, they were polished by SiC abrasive paper from 300 to 800 grits to remove oxides and impurities on the surface, then were dipped into 5% HCl solution for 10 min and rinsed with acetone in ultrasonic bath for 5 min, and finally washed by distilled water. Electrodeposition was carried out in a simple three-electrode electrolytic cell via galvanostatic method. Ti sheet was used as a working electrode and the graphite electrode was used as a counter electrode (spectral grade, 1.8 cm^2). The details of the fabrication of ZnO nanorods, Cu_2O yolk-shell cubes, and PtCu alloy yolk-shell cubes are described as follows:

1) ZnO layers were electrodeposited on Ti substrate in solution of 0.01 M $Zn(NO_3)_2$+0.05 M NH_4NO_3 with current density of 0.4 $mA \cdot cm^{-2}$ at 70 ˚C for 90 min, and its thickness is about 1.5 μm.
2) Cu_2O yolk-shell cubes were electrodeposited on the surface of ZnO layer in solution of 0.015 M $CuCl_2$ +0.68 mM sodium citrate at 0.28mA/cm^2 for 3 h.
3) PtCu alloy yolk-shell cubes were synthesized by immersing the hollow Cu_2O cubes into 20 ml 2 mM H_2PtCl_6 solution that was adjusted pH=4 at 60 ˚C for 1.5 h. During the replacement, ZnO lalyer is dissolved in the acid solution and the PtCu alloy yolk-shell cubes were attached on Ti substrate.

Characterizations: Surface morphologies of the Cu_2O yolk-shell cubes were characterized by field emission scanning electron microscope (SEM, FEI, Quanta 400). Transmission electron microscope (TEM, JEM-2010HR), high resolution TEM (HRTEM, 200 kV) and electron diffraction (ED) were also used to characterize the microstructures of products. The obtained products were also analyzed by X-ray diffraction (XRD, Bruker, D8 Advance) to determine the phases and microstructures. Chemical component analysis was determined by inductively coupled plasma atomic emission spectrometry (ICP-AES) using TJA IRIS(HR) spectrometer.

Electrochemical measurements: Electrocatalytic properties of the prepared PtCu alloy yolk-shell cubes were studied in a stand-ard three-electrode electrolytic cell. A Pt foil served as the counter electrode. A saturated calomel electrode (SCE) with a double salt bridge system was utilized as the reference electrode that was connected to the cell. All potentials used in electrodepo-sition were the values *vs* SCE. The commercial Pt/C catalysts (Johnson Matthey, 20% Pt/C, Vulcan XC-72, Pt nanoparticle size 4 nm) are utilized in this study. PtCu alloy yolk-shell cubes were loaded on the current collectors (Ti sheet, 1.0 cm^2) and then were served as the working electrode. Cyclic voltammetry and chronoamperometry measurements were carried out on a CHI 660D electrochemical workstation (CH instruments, Inc.). Cyclic voltammograms (CVs) for methanol electrooxidation were recorded between -0.2 V and 1.0 V *vs* SCE at a scan rate of 20 mV/s. Chronoamperometry curves for methanol electrooxidation were measured at 0.75 V. For the CV and chronoamperometry measurements of methanol oxidation, an aqueous solution of 0.5 mol/L H_2SO_4+0.5

mol/L CH_3OH was utilized in this study. Prior to all the experiments, the electrolyte solution was purged with high purity N_2 gas for 10 min. All electrochemical measurements were carried out at 25 ^{0}C.

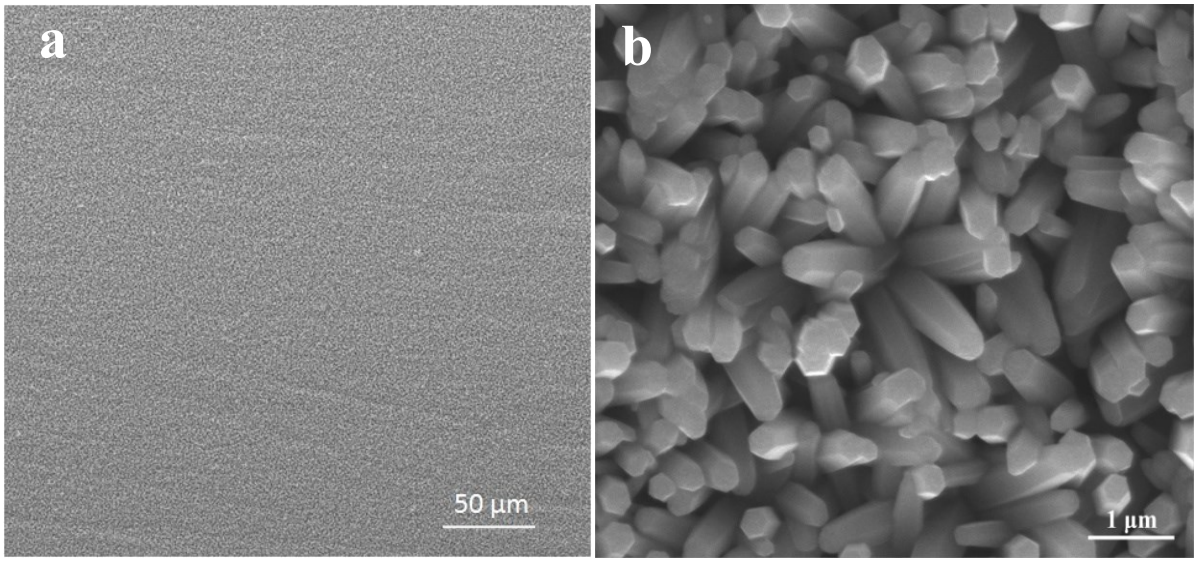

Figure S1. SEM images of ZnO layer with different magnifications electrodeposited on Ti substrate.

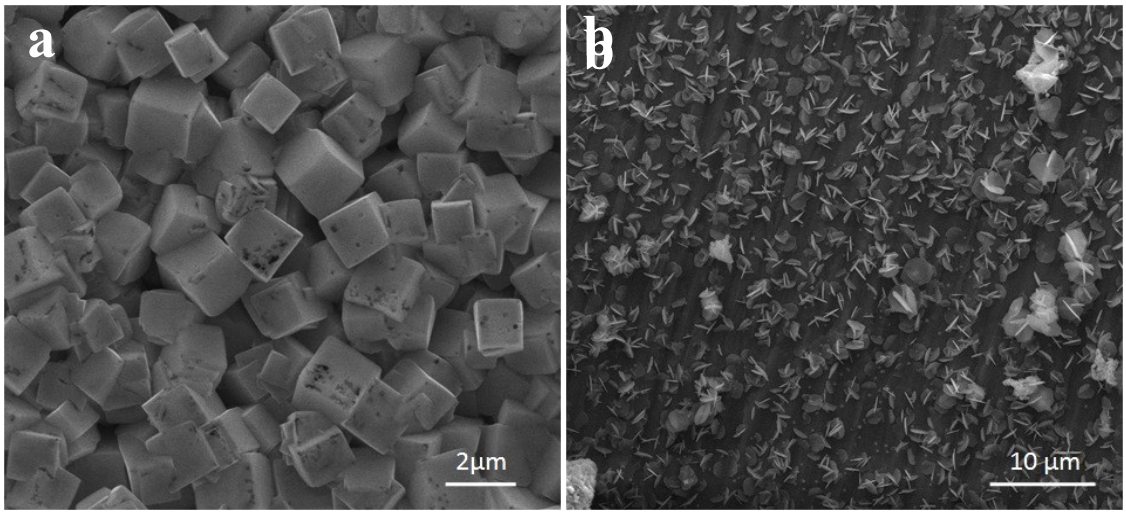

Figure S2. (a) SEM image of well-defined regular Cu_2O cubes electrodeposited on ZnO layer; (b) SEM image of Cu_2O sheets electrodeposited on Ti substrate without ZnO layer.

The formation mechanism of Cu_2O hollow cube

In this study, we combined the influence of Cl^- ions, oriented attachment with Ostwald ripening to well illustrate the formation mechanism of Cu_2O yolk-shell cubes. During this electrodeposition synthesis, besides ZnO layer, the capping effect of chloride ions is also an important factor in directing the formation of hollow Cu_2O cubes. In the presence of Cl^- ions, the Cu^+ ions electroreduced by Cu^{2+} ions could react with Cl^- ions to form intermediate species such as CuCl, which could serve as a reservoir to control the super saturation concentration of Cu^+ ions in solution. As a result, the formation rate of Cu_2O is significantly slowed down, which favours the seeds to grow into individual nanocrystals without aggregation in the early stage of reaction. In addition, M.-J. Siegfried and K.-S. Choi reported that the Cl^- ions can stabilize {100} plane of Cu_2O.[1] According to Bravias law and Wulff principle,[2] the {100} plane growth rate of Cu_2O will be slow down because of Cl^- ions, and eventually {100} plane will be reserved and a cubic crystal will be formed as shown in Figure S3. Then the initially formed cubic crystals with small sizes intend to agglomerate and become large cubes to reduce surface energy (oriented attachment process). Here each cubic nanocrystal is work as a "brick" and the agglomerated solid cube contains dislocations. As the solid cube will continue to grow under the electric field subsequently, so the nanocrystals located on the surface will grow up preferentially because of the surface exposing in solution and accordingly the cubes with smooth surfaces will be formed. With deposition time increasing, the Ostwald ripening happens and leads to dissolution of relatively small nanocrystals in the interior of Cu_2O cube and redeposition on the walls of cube to form Yolk-shell or hollow structures.[3-4] The formation mechanism of Cu_2O Yolk-shell or hollow cube is illustrated in Figure S4a, and it is well proved by the growth process of Cu_2O cube as shown in Figure S4b-d and the evolution process of hollow structures as shown in Figure S4e-g. To demonstrate special role of Cl^- ions in this synthesis, $CuCl_2$ was replaced by $CuSO_4$ or $Cu(NO_3)_2$ (the other conditions were not changed), and here the Cu_2O cubes were not obtained and only Cu_2O spheres were fabricated as shown in Figure S5. Therefore, the role of Cl^- ions in this synthesis is crucial for the formation of Cu_2O

cubes. Based on the evolution process of hollow cube shown in Figure 3e-g, the interior structure of Cu_2O cube could be effectively tailored by control deposition time. The cubes electrodeposited for less 2 h were found to be completely solid as shown in Figure S4e. When electrodeposition time is 3h, the Cu_2O yolk-shell cubes were obtained as shown in Figure S4f. When the electrodeposition time is 4h, the hollow structure is obtained as shown in Figure S4g.

References

[1] H. Wu and W. Chen, *J. Am. Chem. Soc.*, 2011, **133**, 15236.

[2] (a) J. H. D. Donnay and D. A. Harker, *Mineralogist* 1937, **22**, 446; (b) G. Z. Wullf, *Kristallogr Mineral.* 1901, **34**, 449; (c) *J. W. Gibbs, Colle-cted Papers* (*New York*: *Longmans, Green* and *Co.*) *1928*, 154.

[3] (a) C. Kuo and M. H. Huang, *J. Am. Chem. Soc.*, 2008, **130**, 12815; (b) W. Li , Y. Deng, Z. Wu, X. Qian, J. Yang, Y. Wang, D. Gu, F. Zhang, B. Tu and D. Zhao, *J. Am. Chem. Soc.,* **2011**, ***133***, 15830.

[4] H. Xu and W. Wang, *Angew. Chem. Int. Ed.*, 2007, **46**, 1489.

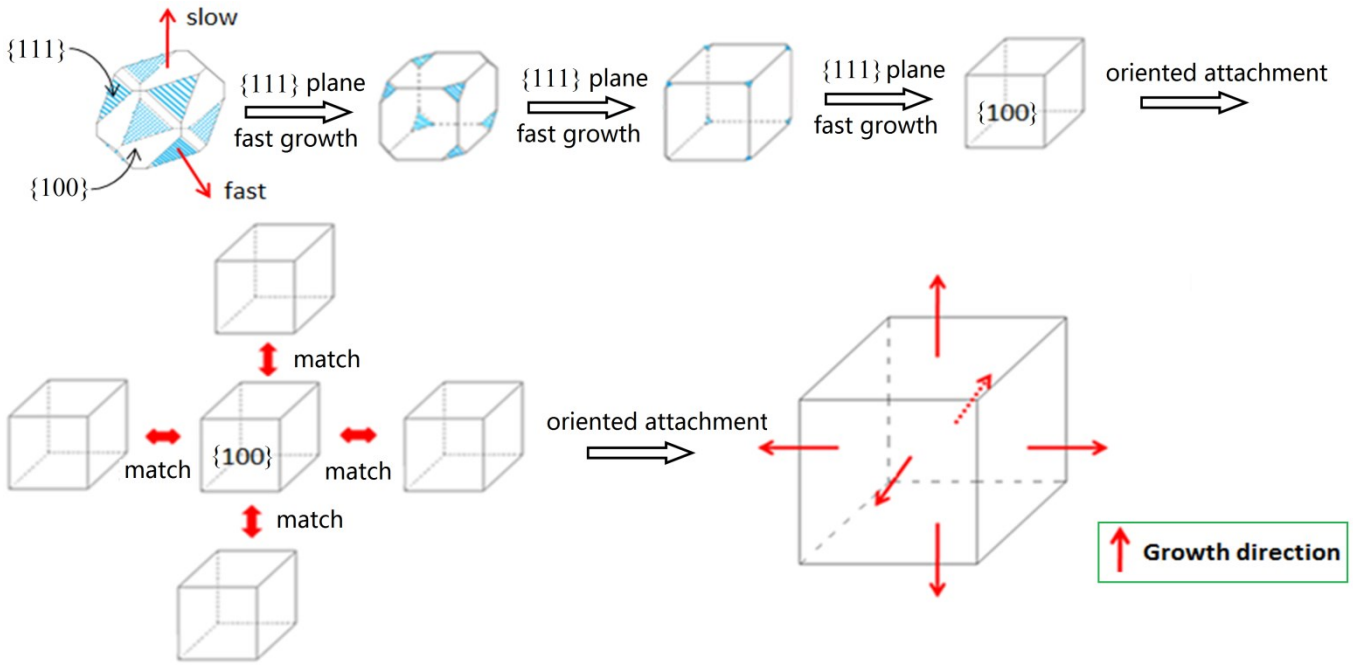

Figure S3. Schematic illustration for the growth process of Cu_2O cubic nanocrystal under the influence of Cl^- ions and the oriented attachment of cubic nanocrystal for the formation of Cu_2O cube.

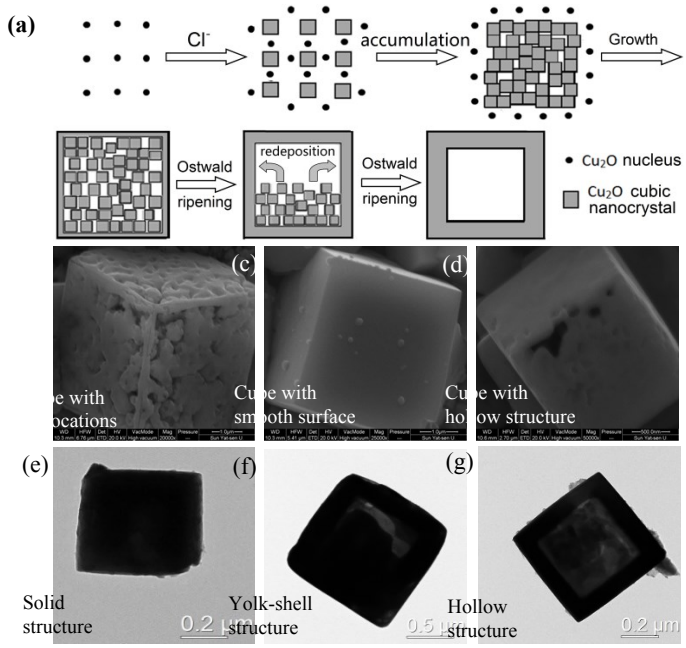

Figure S4. (a) Schematic illustration for the formation mechanism of Cu_2O hollow cube; The evolution of surface morphology of Cu_2O cube from (b)→(c)→(d); The evolution of hollow structure of Cu_2O cube from (e)→(f) →(g) (namely solid structure→yolk-shell structure→hollow structure).

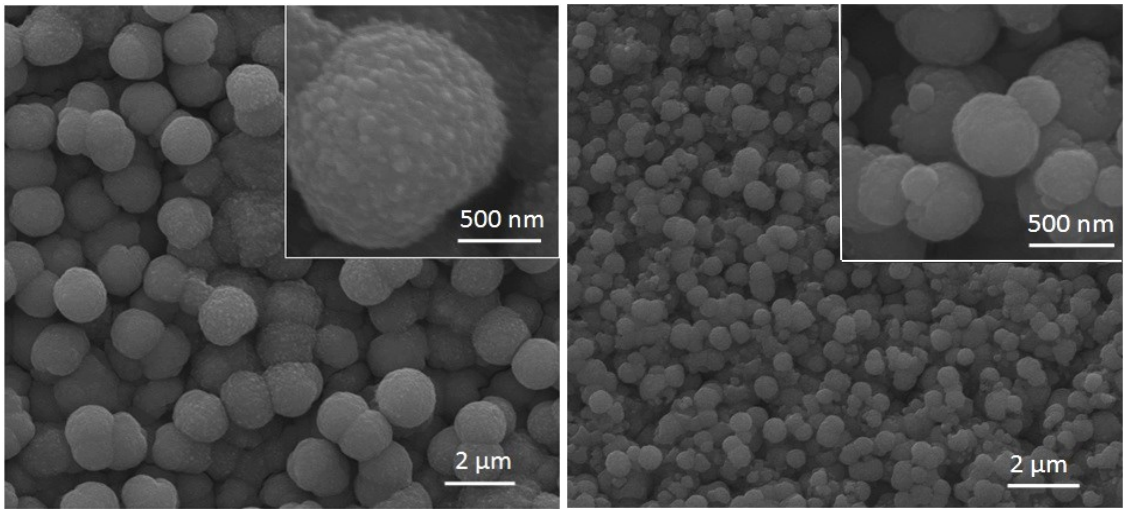

Figure S5. SEM images of the fabricated Cu_2O spherical microparticles when $CuCl_2$ was replaced by (a) $Cu(NO_3)_2$ and (b) $CuSO_4$.

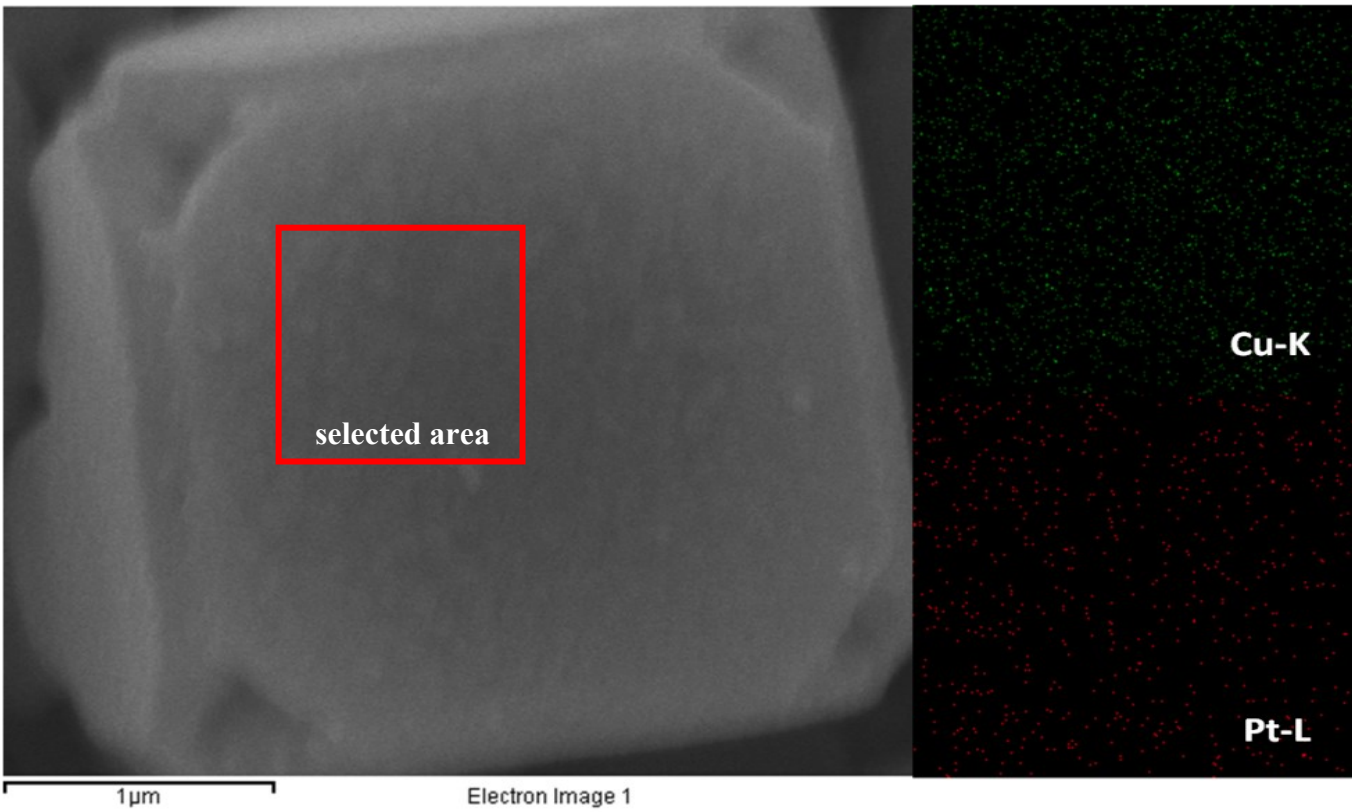

Figure S6. The Pt and Cu element distributions in the Cu_2O yolk-shell cubes.